

# Zwitterionic Copolymers for Anti-Scaling Applications in Simulated Spaceflight Wastewater Scenarios

Elisabeth R. Thomas, Jae Sang Lee, Hoda Shokrollahzadeh Behbahani, Ani Nazari, Yusi Li, Yi Yang, Matthew D. Green, and Mary Laura Lind\*



Cite This: *ACS Omega* 2023, 8, 18462–18471



Read Online

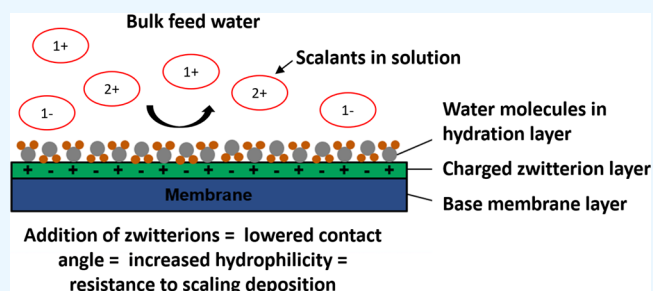
ACCESS |

Metrics & More

Article Recommendations

Supporting Information

**ABSTRACT:** Water reclamation in spaceflight applications, such as those encountered on the International Space Station (ISS), requires complex engineering solutions to ensure maximum water recovery. Current vapor compression distillation (VCD) technologies are effective but produce highly concentrated brines and often cause scaling within a separation system. This work evaluates initial steps toward integrating pervaporation, a membrane separation process, as a brine management strategy for ISS wastewaters. Pervaporation performs separations driven by a chemical potential difference across the membrane created by either a sweep gas or a vacuum pull. Pervaporation membranes, as with most membrane processes, can be subject to scaling. Therefore, this work studies the anti-scaling properties of zwitterions (polymeric molecules with covalently tethered positive and negative ions) coated onto sulfonated pentablock terpolymer block polymer (Nexar) pervaporation membrane surfaces. We report a method for applying zwitterions to the surface of pervaporation membranes and the effect on performance parameters such as flux and scaling resistance. Membranes with zwitterions had up to 53% reduction in permeance but reduced scaling. The highest amount of scaling occurred in the samples exposed to calcium chloride, and uncoated membranes had weight percent increases as high as  $1617 \pm 241\%$ , whereas zwitterion-coated membranes experienced only about  $317 \pm 87\%$  weight increase in the presence of the same scalant.



## 1. INTRODUCTION

Pervaporation is a membrane process that utilizes dense, non-porous membranes to perform separations driven by a chemical potential difference. Pervaporation membranes are generally made from dense polymers or molecular sieving inorganic materials. Membrane materials may be relatively more hydrophilic or hydrophobic, depending on the solute of interest and desired separation in a system.<sup>1</sup> Pervaporation operates via a difference in chemical potential between the feed and permeate sides of the membrane, often realized by applying a vacuum to or passing a sweep gas by the permeate side of the membrane, and then condensing the vapor in the permeate later in the process.<sup>2</sup> The current hypothesis on solvent transport through pervaporation membranes is that it occurs via a solution-diffusion mechanism based on solubility of and diffusion through the dense structures, not convective flow through open pores.<sup>3</sup> One of the most advantageous aspects of pervaporation, compared to applied pressure driven processes such as reverse osmosis, is that pervaporation is not limited by the total dissolved solids (TDS) of the feed (maximum  $\sim 80 \text{ g L}^{-1}$  for RO processes).<sup>4</sup> Pervaporation has advantages over processes such as membrane distillation (MD) as well. MD utilizes porous membranes, which are subject to failure through wetting, where liquid solvent enters the pores

of a membrane and destroys its ability to perform separation through convective gas flow.<sup>5</sup> The dense nature of pervaporation membranes makes them impervious to wetting and allows them to retain volatile organic compounds based on their solubility (or lack thereof) in the polymer.<sup>5</sup> While highly contaminated feeds can still pose challenges, such as scaling or fouling, the pervaporation process has the potential of handling feeds with both organic and inorganic contaminants.<sup>6–8</sup>

Scaling is a phenomenon in water treatment systems wherein inorganic species deposit onto the surface of the equipment or membranes which can cause systematic problems with performance.<sup>9</sup> Fouling, similar to scaling, is when organic materials deposit in a system.<sup>10</sup> In membrane systems, scaling frequently occurs on the surface of the membrane, which will gradually reduce flux and eventually cause the process to fail.<sup>11,12</sup> Scaling can be initiated by precipitates forming in the bulk of the solution or at the

**Received:** December 23, 2022

**Accepted:** April 26, 2023

**Published:** May 15, 2023



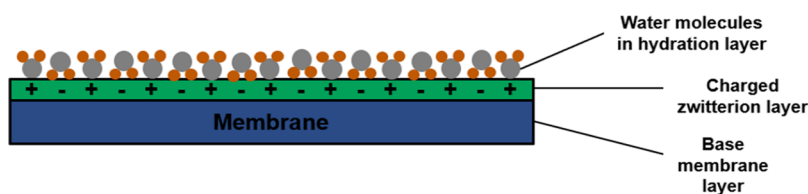


**Figure 1.** Depiction of the zwitterion-coated membrane and accompanying hydration layer theorized to provide anti-scaling properties to surface interfaces.

membrane–feed interface.<sup>13</sup> One way to enhance scaling resistance is to increase the hydrophilicity of the membrane, which is theorized to “hold” a hydration layer of water molecules on the surface of the membrane and either slow or mitigate scalant nucleation, depicted in Figure 1.<sup>14,15</sup> Zwitterions are polymeric molecules with covalently tethered positive and negative ions, but an overall neutral charge and zwitterion coatings increase the hydrophilicity of membrane surfaces.<sup>14–17</sup> Liu et al. and Davenport et al. showed that the increase in surface hydrophilicity from the addition of zwitterion to a membrane surface makes it difficult for scalants to deposit and increases the lifetime of the membrane.<sup>17,18</sup>

The urine processing assembly (UPA) used on the International Space Station (ISS) often experiences scaling from the highly concentrated wastewaters.<sup>19</sup> Currently, the ISS uses vapor compression distillation (VCD) to recycle wastewaters, primarily composed of urine products, on the station.<sup>19</sup> However, one of the main challenges facing the VCD of water processing is scaling through solid build up in the system. Currently, the VCD produces a maximum of 70% recovery, necessitating the handling, storage, and disposal of leftover brine.<sup>20</sup> The National Aeronautics and Space Administration (NASA) desires a minimum water recovery of 85%.<sup>21</sup> Generally, in water treatment processes, and specifically for NASA and the ISS, divalent ions (e.g.,  $\text{Ca}^{2+}$  and  $\text{Mg}^{2+}$ ) are of particular concern because of the potential for scaling. NASA is planning for long-term missions within the next decade with little or no possibility of resupply from earth (Artemis, Gateway, and potentially Mars); therefore, improved methods of purifying water with high recovery are mission critical. Astronauts will need in situ methods of resource reclamation rather than relying on re-supply missions.

Our group has previously demonstrated that sulfonated block polymers, tradename Nexar, performed well as pervaporation desalination membranes, with water permeances as high as  $135 \text{ kg m}^{-2} \text{ h}^{-1} \text{ bar}^{-1}$ .<sup>22</sup> Nexar forms microstructures within a finalized polymer product because of the nature of the hydrophilic and hydrophobic components of the polymer backbone. These microstructures are influenced by the composition (ratio of polar to non-polar solvent) of the solvent used to process the polymer. Other groups have performed extensive investigations into how these changes occur.<sup>23</sup> In our previous Nexar work for pervaporation desalination, we found that casting membranes at ratios of 10–50 wt % of *n*-propanol to toluene did not yield a statistically significant difference in separation performance.<sup>22</sup> Microstructures are important to understand membranes made from the Nexar polymer as they can change throughout a process. Previously published studies by Truong et al. found that exposure to water and drying cycles can substantially stress the Nexar microstructures within the polymer and cause them to go from ordered to disordered.<sup>23,24</sup> These changes can have significant impacts on the final performance and processability

of the membranes due to increased brittleness and lowered flexibility.

This is the first report of a method to coat pervaporation Nexar membranes with zwitterions and the subsequent separation performance and scaling resistance properties. Our zwitterion modifications enhanced the roughness and relative hydrophilicity of the membrane surface (contact angle of the bare Nexar membrane is  $89.9^\circ \pm 9.9$  and contact angle of the zwitterion-coated membrane is  $22.3^\circ \pm 10$ ) and significantly decreased the amount of surface scaling on the membranes. The highest amount of scaling occurred in the samples exposed to calcium chloride, and uncoated membranes had weight percent increases as high as  $1617 \pm 241\%$ , whereas zwitterion-coated membranes experienced only about  $317 \pm 87\%$  weight increase under the same testing conditions. As expected, the extra thickness of the zwitterion coating adds increased transport resistance to the coated membranes which is reflected in a lower observed water passage. However, the improved anti-scaling properties showed potential to enhance the lifetime of the membrane system and yield high recoveries over time.

## 2. MATERIALS

Kraton Polymers LLC, Houston, TX, USA, generously provided Nexar polymer, in a solvent mixture of cyclohexane and heptane, with an ion exchange capacity (IEC) of  $2.0 \text{ meq g}^{-1}$ . We purchased commercial Mylar sheets (poly(ethylene terephthalate) (PET)) type F-50043 from the Griff Network for casting. We purchased toluene, *n*-propanol, tetrahydrofuran (THF), hydroxyethylmethacrylate (HEMA), dimethyl sulfoxide (DMSO), azobisisobutyronitrile (AIBN), poly(ethylene glycol) diacrylate 500 Mn (PEGDA), [2-(methacryloyloxy)ethyl]dimethyl-(3-sulfopropyl)ammonium hydroxide (DMAPS), 2,2-dimethoxy-2-phenylacetophenone (DMPA), 2-hydroxy-2-methylpropiophenone (HOMPP), sodium chloride, ammonium bicarbonate, potassium sulfate, monopotassium phosphate, magnesium chloride, and calcium chloride from Sigma-Aldrich. We obtained DRIERITE gypsum desiccant with indicator from Drierite.com.

## 3. METHODS

**3.1. Membrane Synthesis Procedures.** **3.1.1. Nexar Membrane Preparation.** We synthesized Nexar membranes based on a slightly modified procedure from our previously published research.<sup>22</sup> In that work, we found that 11 wt % Nexar dissolved in 50/50 wt % *n*-propanol and toluene cast with a doctor blade at a height of  $200 \mu\text{m}$  had the highest permeance at  $135 \text{ kg m}^{-2} \text{ h}^{-1} \text{ bar}^{-1}$ .<sup>22</sup> When we coated these initial Nexar membranes with zwitterions (described below), we found that the disparity in swelling rates between the zwitterion coating and the base Nexar membrane resulted in the membranes rupturing during cross-flow pervaporation testing at a vacuum level of  $\sim 10^{-4}$  torr. Therefore, for this

study, we made solutions of 20 wt % Nexar in 50/50 wt % *n*-propanol/toluene, cast with a doctor blade at a height of 400  $\mu\text{m}$  on a Mylar sheet. We thoroughly dry these membranes in the fume hood to ensure no residual solvent exists in the membrane, and we are left with strictly polymer. When we coated these membranes with zwitterions as described below, we found that they did not rupture in our cross-flow pervaporation system.

**3.1.2. Zwitterion Coating Method.** We tested several different copolymerization methods for incorporating the zwitterion [2-(methacryloyloxy)ethyl]dimethyl-(3-sulfopropyl)ammonium hydroxide (DMAPS) onto the surface of the Nexar membranes; see the [Supplementary Information \(SI\)](#) for unsuccessful methods. We developed a solvent-free method in which we initiated a reaction between [2-(methacryloyloxy)ethyl]dimethyl-(3-sulfopropyl)ammonium hydroxide (DMAPS) and PEGDA using radical photoinitiator, HOMPP. [Figure 2](#) shows the chemical structure of these four

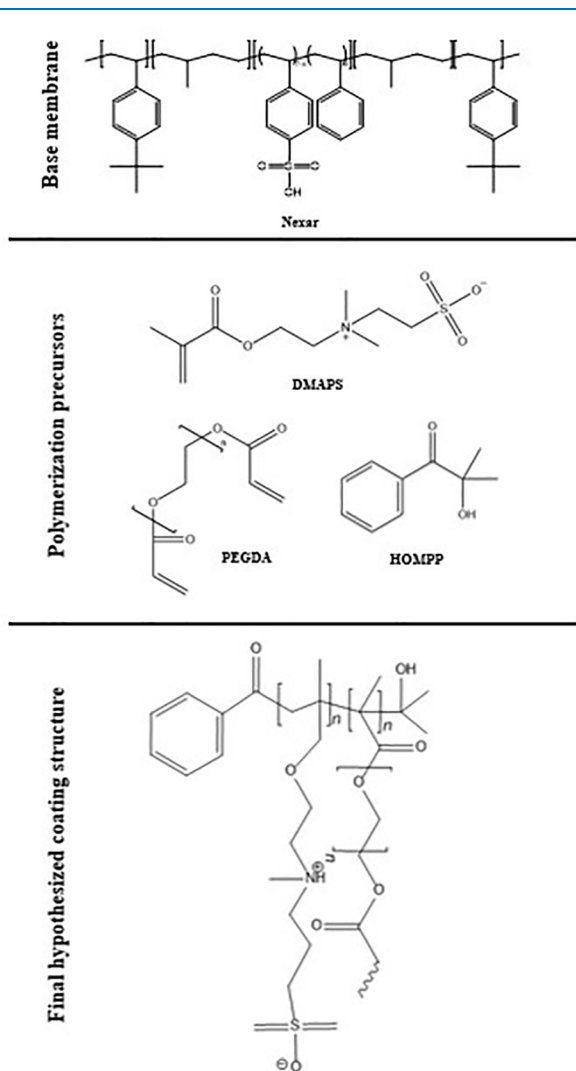


**Figure 2.** Polymer structures used in anti-scaling membrane development and a theoretical final structure of the coating polymer. Nexar is the base polymer layer and unchanged throughout the process. DMAPS is the zwitterion of interest, PEGDA serves as a monomer to accomplish copolymerization with, and HOMPP is the UV activated free radical initiator. The final structure is theorized at the bottom of the figure.

macromolecules. PEGDA, the polymer used in the copolymerization reaction, is in the liquid state at standard conditions and has two double carbon bonds, which serve as a site for free radical initiated polymerization. DMAPS, the zwitterion, is in the solid state and also has a double carbon bond. The double carbon bonds provide sites where free radical initiation occurs.

To prepare the zwitterion coating on the Nexar membranes, we made a batch of 15 grams of solution containing 50 mol % PEGDA and 50 mol % DMAPS. We added the DMAPS powder to the PEGDA liquid in a scintillation vial and stirred at 3000 rpm for 1 h at room temperature. Next, we added HOMPP (as an initiator) to the scintillation vial for a target of 3.7 mol %. Next, we wrapped the vial in foil to prevent ambient light from inducing photoinitiation and stirred for 1 h at room temperature. Then, we poured approximately 3 mL of the PEGDA/DMAPS/HOMPP solution onto the Nexar membrane and cast with the doctor blade at a height of 200  $\mu\text{m}$ . Finally, we placed the Nexar membrane coated with PEGDA/DMAPS/HOMPP to cure in the UV chamber (36 W and 365 nm) for 10 min at a distance of three inches from the light source. After curing, we removed the coated membranes from the Mylar sheet for testing.

For membrane coupons tested in our pervaporation cross-flow system, we coated zwitterions onto one side of the membrane; for membrane coupons tested in the passive scaling batch tests, we coated zwitterions onto both sides of the membranes to obtain a uniform surface for monitoring scalant deposition.

**3.1.3. Membrane Post-Treatment Methods.** In polymeric membrane processes, there is often a post-treatment step such as a rinse in deionized (DI) water or other solution, sometimes coupled with sonication to remove excess unreacted monomers from the membrane.<sup>25</sup> For these membranes, we explored sonication of membranes in DI water to check for excess monomer removal, additional information on this process can be found in the [SI](#). For sonicated samples, we sonicated the membranes for 15 min in 100 mL of ultrapure DI water and then decanted the water from the tube; we repeated DI water rinsing three times. We performed this for both as-cast Nexar membranes and Nexar membranes coated with zwitterions. After sonication washing of the membranes, we placed the membranes in a desiccator vacuum jar to dry and store until use. We prepared four general types of membranes, summarized in [Table 1](#).

**Table 1.** Membrane Sample Types Including Casting and Treatment Variables Used for Later Analysis

sample ID	sample description	coating	sonication
UN	Nexar untreated	none	no
SN	Nexar sonicated	none	yes
UZ	zwitterion untreated	zwitterion copolymer	no
SZ	zwitterion sonicated	zwitterion copolymer	yes

**3.2. Membrane Characterization Procedures.** **3.2.1. Attenuated Total Reflectance Fourier Transform Infrared (ATR-FTIR) Spectroscopy.** We measured ATR-FTIR spectra using a Nicolet 6700 FTIR machine with a Smart Orbit diamond ATR attachment, taking 32 scans per sample. We performed this analysis on membrane sample types (Nexar sonicated (SN) and Nexar zwitterion-coated sonicated (SZ)).

**3.2.2. Contact Angle.** We collected DI water contact angles using a Kruss Easy Drop contact angle goniometer in sessile

drop mode. We measured 10 drops per sample for both Nexar untreated (UN) and Nexar zwitterion-coated (UZ) sample types, removing both the highest and lowest measurements for each. We did not perform contact angle measurements on sonicated samples, SN and SZ, because the membranes would not lie flat on the goniometer plate.

**3.2.3. Surface Roughness Measurements.** We performed surface roughness measurements using a Zygo ZeScope optical profilometer on both zwitterion-coated samples and base Nexar samples. For each sample type, we used three different membranes from different castings to ensure a variety of samples for a total of six samples altogether. The zwitterion-coated membranes have incredibly rough surfaces and necessitated some individual adjustments to the equipment for each sample loading. For zwitterion samples, we used a zoom of 12.48 magnification and took sample areas over an average area of  $0.35 \pm 2.2 \times 10^{-3} \text{ mm}^2$ , with the varied sample size from equipment adjustment as we loaded new samples on to the machine. For Nexar samples, which have a much smoother surface overall, we used a zoom of 3.16 magnification and took sample areas over a set area of  $1.67 \text{ mm}^2$ .

**3.2.4. Soxhlet Extraction for Extent of Polymerization.** We performed a Soxhlet extraction analysis to analyze the extent of polymerization of the unsupported zwitterion polymer. We made free-standing zwitterion layers as described in Section 3.1.2 without the base Nexar membrane. We ran the extraction process for 24 h in THF and dried the samples in a vacuum oven at ambient temperature post extraction. We took initial and final weights of the polymers in order to determine the gel fraction (extent of polymerization) experienced by the polymer. Gel fraction is calculated according to eq 1.

$$G = \left( \frac{W_{\text{fin}}}{W_{\text{init}}} \right) \times 100 \quad (1)$$

where  $G$  is the gel fraction and is unitless, often expressed as a percentage. The terms  $W_{\text{init}}$  and  $W_{\text{fin}}$  (g) represent the initial and final weights of the polymer sample, respectively.

**3.3. Membrane Performance Procedures.** **3.3.1. Pervaporation Flux Experiments.** We performed pervaporation flux experiments following standard procedures previously published by our research group using our custom-built cross-flow cell with a membrane active area of 5 cm by 5 cm, a recirculating feed, a vacuum level of  $\sim 10^{-4}$  torr, and a liquid nitrogen cold trap to capture the permeate.<sup>22</sup> We placed membranes into the pervaporation cross-flow cell and performed leak tests (consisting of circulating water and draining twice) for 30 min with DI water and high vacuum ( $\sim 10^{-4}$  torr). We tested zwitterion-coated membranes in the pervaporation cross-flow cell that only had zwitterions coated on the feed side of the membrane (and not both sides, as the membranes which were tested in passive scaling tests). If we did not detect any leaks, we then changed the feed water to a  $32 \text{ g L}^{-1}$  sodium chloride solution and operated the system with the high vacuum for 30 min to achieve steady state operation. After the initial equilibration time, we collected the permeate for 30 min and analyzed its mass through gravimetric analysis. We measured the conductivity of the permeate using an EDAQ (Colorado Springs, CO) USB isoPod EPU357 conductivity meter to calculate the salt removal value.

From the raw data collected (time, mass, and conductivity), we calculated membrane flux, permeance, and salt removal.

Flux is the passage of water through the membrane over a given time normalized by the area of the membrane.

$$J_{\text{water}} = \frac{m}{A \Delta t} \quad (2)$$

where  $J_{\text{water}}$  ( $\text{kg m}^{-2} \text{ h}^{-1}$ ) is the flux,  $m$  (kg) is the mass of water collected,  $A$  ( $\text{m}^2$ ) is the active area of the membrane, and  $\Delta t$  (h) is the time over which we collected the mass. Permeance,  $F_{\text{water}}$  ( $\text{kg m}^{-2} \text{ h}^{-1} \text{ bar}^{-1}$ ), is the flux normalized by the difference in vapor pressures between the feed and permeate sides of the membrane. Permeance enables easy comparisons across membranes of different materials tested at variable operating conditions.

$$F_{\text{water}} = \frac{m}{A \Delta t \Delta p^{\text{sat}}} \quad (3)$$

where  $\Delta p^{\text{sat}}$  (bar) is the difference in vapor pressure between the permeate and feed sides of the membrane, and  $A$ ,  $m$ , and  $\Delta t$  are as described for eq 2. Permeability,  $P_{\text{water}}$  ( $\text{kg m m}^{-2} \text{ h}^{-1} \text{ bar}^{-1}$ ), is related to permeance but also normalizes for the thickness of a membrane in the system to allow comparisons across different membrane types.

$$P_{\text{water}} = \frac{ml}{A \Delta t \Delta p^{\text{sat}}} \quad (4)$$

where all variables are as defined above and  $l$  (m) is the membrane thickness. Finally, salt removal is the measure of the efficacy of a given separation.

$$R_{\text{salt}} = \left( 1 - \frac{c_{\text{perm}}}{c_{\text{feed}}} \right) \times 100 \quad (5)$$

In eq 4,  $R_{\text{salt}}$  is the salt removal value and is unitless, often expressed as a percentage. The terms  $c_{\text{perm}}$  and  $c_{\text{feed}}$  ( $\text{g L}^{-1}$ ) represent, respectively, the salt concentrations in the permeate and feed streams. We generated calibration curves using standardized solutions prior to each conductivity measurement in order to ensure accurate readings.

**3.3.2. Passive Scaling Test Protocol.** We performed passive scaling studies on the membranes in static, batch solutions. We chose to run these scaling studies in a passive environment given that the eventual goal of this vein of research is to utilize a passive treatment system that does not implement any energy inputs and, therefore, does involve the stagnant deposition of scalant species on to the surface of the membrane. The goal of isolating each component was to allow us to gain a greater understanding of how each species would behave in regard to scalant surface deposition and growth. We placed membranes in scaling solutions and used gravimetric analysis to quantify the mass of scalant deposited on the membranes over a one-week period. Table 2 shows the synthetic scaling solutions of individual scalants of interest to NASA that we made at room temperature in DI water and used for these studies.<sup>26</sup>

For the scaling experiments, we placed 70 mL of each scalant solution into a plastic 100 mL jar with a lid with a single membrane coupon ( $\sim 2.5 \times 7 \text{ cm}$ ) and allowed it to sit, sealed for 1 week at room temperature. One week is selected as the timeline to reflect the length we anticipate a passive separation process utilizing these membranes occurring. We performed triplicate experiments of each type of coated and uncoated membrane. After removal from the solution, we placed the membranes in a desiccant vacuum sealed chamber until dry.

**Table 2. Scalant Solution Concentrations<sup>a</sup>**

scalant name	chemical formula	concentration (g L <sup>-1</sup> )
ammonium bicarbonate	NH <sub>5</sub> CO <sub>3</sub>	217
sodium chloride	NaCl	359
potassium sulfate	K <sub>2</sub> SO <sub>4</sub>	111
monopotassium phosphate	KH <sub>2</sub> PO <sub>4</sub>	226
magnesium chloride	MgCl <sub>2</sub>	546
calcium chloride	CaCl <sub>2</sub>	754

<sup>a</sup>Scalant solutions were made at the solubility limit for each species as measured at 20 °C.

Once dry, we measured the final membrane mass and calculated the percent weight change of the membranes.

To ensure a homogeneous sample, coated membranes had coatings on both sides of the membrane although this is not necessary for pervaporation system implementation. This allowed the samples to free-float in the scaling solution without exposing both Nexar and zwitterion-coated sides of the membrane to the scalants. In system implementation, it is only necessary for the feed side of the membrane to be coated as that is the only side in contact with scalants. NASA is interested in passive systems which leverage existing operations on the space station, and therefore, we chose to evaluate passive scaling of the membranes (without external inputs such as a cross-flow feed pump or a vacuum pump on the permeate side).<sup>27</sup>

## 4. RESULTS AND DISCUSSION

### 4.1. Membrane Characterization. 4.1.1. ATR-FTIR Analysis of Nexar Structure in Various Processing Stages.

The results of the ATR-FTIR performed on the Nexar polymer before and after sonication steps reveal that no chemical structure changes take place. When sonicating the membrane prior to passive scalant studies, it is necessary to include a desiccation step to be able to accurately take the weight of the membrane prior to submersion in the scalant solution. This wetting/drying cycle does change the microstructure, leading to significant mechanical changes. While Nexar in its freshly cast state is flexible and facile to handle, the wet-dry cycling experienced during the sonication/desiccation process yields a brittle membrane that breaks very easily as described by Truong et al.<sup>23,24</sup> This change in microstructure and mechanical properties makes the sonicated Nexar membrane unsuitable for use in a system.

In order to further probe the changes seen after sonicating the membranes, we investigated the bond structure of membranes in various states of processing. Figure 3 shows the ATR-FTIR spectra for the dried, as-received Nexar polymer and the cast membranes. While there is a difference in intensity in the peaks across all samples, there are no bond shifts or changes indicating that sonication does not change the chemical bonding of the Nexar membranes. Differences in intensity suggest that differing amounts of materials are present in each sample and/or poor contact with the machine.

**4.1.2. ATR-FTIR Analysis of the Membrane Coating Procedure.** When performing the polymerization procedure on the surface of the membranes, the PEGDA acts as the solvent for the DMAPS; as a solvent-free process, this minimized the potential dissolution or swelling of Nexar (which occurs in certain solvents, e.g., *n*-propanol, toluene, heptane, cyclohexane, water, etc.). HOMPP, the polymerization initiator, is also liquid. This solvent free process can

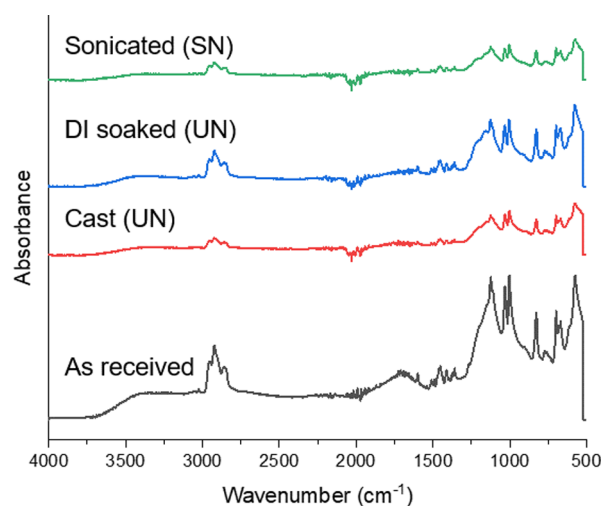


**Figure 3.** FTIR-ATR spectra for Nexar as-received polymer and cast membranes in various states of processing. The as-received polymer arrives in a solution of cyclohexane and heptane, and we dried the polymer in order to remove the hydrocarbons. The UN cast membrane is an unsonicated Nexar membrane after casting according to protocols outlined in Section 3. DI soaked and sonicated membranes are processed as mentioned above. While peak intensity varies, there are no significant peak changes that suggest bond structure change.

provide a fast polymerization reaction. Figure 4 shows the ATR-FTIR spectra of the polymer components and coated membrane. In the component materials, the C=O peak is present at 1720 cm<sup>-1</sup> in PEGDA, 1664 cm<sup>-1</sup> in HOMPP, and

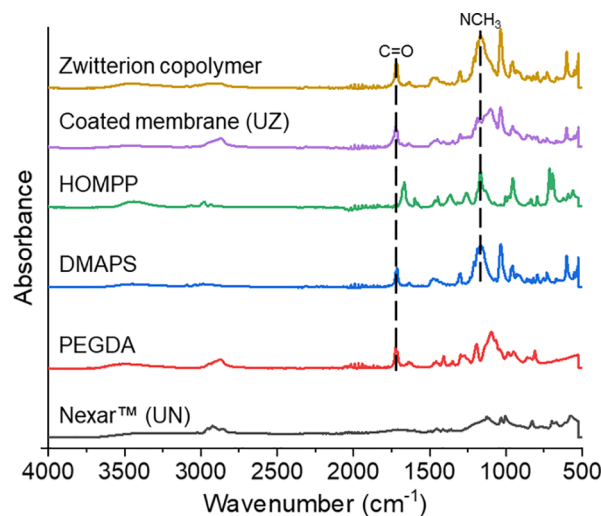


**Figure 4.** ATR-FTIR analysis of each constituent of the membrane synthesis process as well as the final coated membrane. The representative peaks marked on the graph present in polymerization precursors and the final coated membrane indicate that the desired polymerization reaction occurred and that the zwitterion copolymer is present on the surface of the membrane. In the component materials, the C=O peak is present at 1720 cm<sup>-1</sup> in PEGDA, 1664 cm<sup>-1</sup> in HOMPP, and 1714 cm<sup>-1</sup> in DMAPS. There is no C=O functionality in Nexar. Therefore, the peak at 1722 cm<sup>-1</sup> on the UZ (Nexar coated with zwitterion) indicated successful zwitterion polymerization. Additionally, the NCH<sub>3</sub> peaks at 1163 cm<sup>-1</sup> in DMAPS, 1169 cm<sup>-1</sup> in HOMPP, and very strongly at 1161 cm<sup>-1</sup> in the final coating structure further support this polymerization taking place as desired.

1714  $\text{cm}^{-1}$  in DMAPS.<sup>28</sup> There is no C=O functionality in Nexar. Therefore, the peak at 1722  $\text{cm}^{-1}$  on the UZ (Nexar coated with zwitterion), as well as the zwitterion copolymer with no Nexar base, indicates that the zwitterion polymerization was successful. The triple peak at just below 3000  $\text{cm}^{-1}$  is indicative of CH stretching occurring throughout the polymer matrix; this stretching is less visible or absent in the coated samples. Peaks slightly to the left of the of the 1000  $\text{cm}^{-1}$  line indicate the presence of the sulfur functional groups on the Nexar polymer.<sup>29</sup> The final polymerized coating C=O peak appears at 1722  $\text{cm}^{-1}$ , which is shifted higher than the three individual polymerization components, and suggests that desired polymerization took place because of the appearance C=O bonds in the final coated membrane structure which are not present in the base Nexar membrane. Additionally, the  $\text{NCH}_3$  peak at 1163  $\text{cm}^{-1}$  in DMAPS, 1169  $\text{cm}^{-1}$  in HOMPP, and very strongly at 1161  $\text{cm}^{-1}$  in the final coating structure further support desired zwitterion polymerization. This peak is somewhat spread out in the spectra for the sample with the coating on the base Nexar, likely due to the hydrogen bonding both within the polymer matrix and between the coating and the base membranes. Figure 2 shows the hypothesized final structure of the zwitterion coating. The shifting of the absorbance of carbonyl in the final structure (1722  $\text{cm}^{-1}$ ) suggests stretching, potentially because the final structure is experiencing overlapping stresses within the polymer matrix. Polymerization is random, and therefore, there are a myriad of possible configurations of the final copolymer structure. For example, the HOMPP initiator splits into two free radicals when exposed to UV light, so either one of those molecules could serve to initiate or terminate the molecule.<sup>30,31</sup> While the DMAPS and PEGDA were mixed in equimolar ratios, it is nearly impossible for the structure to perfectly alternate the molecules, hence the brackets in Figure 2 that can denote different amounts of each molecule. Some polymerization occurs from the second carbon double bond in the PEGDA molecule, indicated by a wavy line in Figure 2, therefore creating a non-linear polymer structure. The two vinyl groups on PEGDA can serve as polymerization sites, both for copolymerization with the DMAPS polymer as well as crosslinking within the polymer matrix and polymerization between PEGDA/PEGDA molecules. Given the nature of the underlying Nexar polymer and the coating, we hypothesize membrane bonding occurs due to physical adhesion between the two layers.

**4.1.3. Contact Angle Analysis.** Figure 5 shows the average contact angles and a representative photo for the UN and UZ membranes. The average contact angle for the UN membranes (bare Nexar membranes) was  $89.9^\circ \pm 9.9^\circ$ , which was larger than the average contact angle for UZ membranes (zwitterion-coated) which was  $22.3^\circ \pm 10.1^\circ$ . The zwitterion coating on the UZ sample reduces the DI water contact angle of the membrane surface, indicating that the zwitterion functionality is present on the membrane and is inducing relative hydrophilicity. Since scaling at the membrane surface is a primary concern in system scaling, surface interactions are of significant importance. Increased relative hydrophilicity is shown to assist in enhancing anti-scaling properties.<sup>32</sup> Commercially available polyvinyl alcohol (PVA) pervaporation membranes (DeltaMem 4155-30) are used as a benchmark. Previous reports on these membranes show a lower hydrophilicity, with the average contact angle around  $60^\circ$ . Therefore, both our Nexar and zwitterion membranes have larger contact

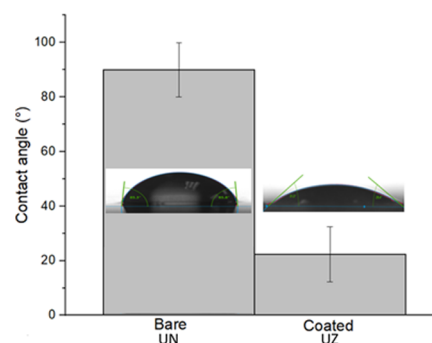


**Figure 5.** Contact angle values for UN (bare) and UZ (zwitterion-coated) membrane samples in deionized water with representative pictures of each contact angle. The coated membrane shows an increase in hydrophilicity correlating with a decrease in contact angle. Increased hydrophilicity is theorized to assist in enhancing anti-scaling properties.

angles than commercially available PVA pervaporation membranes.<sup>33</sup>

**4.1.4. Surface Roughness Measurements.** The surface roughness measurements we took yielded significant differences between the zwitterion-coated membranes and the Nexar membranes. The average roughness of the zwitterion membranes across three different samples was  $9.95 \pm 1.3 \mu\text{m}$  measured as root mean square (RMS). The Nexar surface roughness average across three samples was  $0.0939 \pm 0.067 \mu\text{m}$  as RMS. The zwitterion-coated membranes have larger surface roughness than the Nexar membranes. Our zwitterion membranes had enhanced hydrophilicity, even with the increase in surface roughness.

Studies performed by Lin et al. and Shaffer et al. show that surface roughness can be correlated with an increase in gypsum scaling propensity on polymeric surfaces, but that scaling behavior is impacted by a number of factors, including surface chemistry.<sup>34,35</sup> In Section 4.2.3 below, we found that our zwitterion membrane had lower scaling propensity than uncoated membranes despite the increase in surface roughness of the zwitterion membranes, agreeing with the previous studies that many factors can impact scaling behavior in membrane systems.

**4.1.5. Soxhlet Analysis of Polymerization.** The analysis of Soxhlet extraction revealed a gel fraction of the polymer of  $94.7\% \pm 1.5\%$ . This indicates that the polymerization took place as desired and created the polymer matrix between the DMAPS, PEGDA, and HOMPP constituents in alignment with the ATR-FTIR results. A gel fraction of  $>90\%$  is considered desirable to obtain well polymerized samples with minimal leftover constituents.

**4.2. Membrane Performance Testing.** **4.2.1. Pervaporation Flux and Desalination Experiments.** Table 3 shows the cross-flow pervaporation desalination tests of membrane performance. The bare Nexar membranes (UN) had a permeance of  $122.1 \text{ kg m}^{-2} \text{ h}^{-1} \text{ bar}^{-1} \pm 5.1 \text{ kg m}^{-2} \text{ h}^{-1} \text{ bar}^{-1}$ , and the coated membranes (UZ) had a permeance value of  $63.9 \text{ kg m}^{-2} \text{ h}^{-1} \text{ bar}^{-1} \pm 8.7 \text{ kg m}^{-2} \text{ h}^{-1} \text{ bar}^{-1}$ . Under a one-way analysis of variance (ANOVA) statistical test (with an alpha value of 0.05 and a Tukey means comparison), the difference in permeance between the Nexar membranes, regardless of casting method, was not statistically significant.<sup>22</sup> We chose not to test the SN membrane due to the brittleness induced by the sonication step making those samples non-

**Table 3. Membrane Thickness, Flux, Permeance, and Permeability for Various Membrane Sample Types**

sample type	membrane thickness ( $\mu\text{m}$ )	flux ( $\text{kg m}^{-2} \text{h}^{-1}$ )	permeance ( $\text{kg m}^{-2} \text{h}^{-1} \text{bar}^{-1}$ )	permeability ( $\text{kg m m}^{-2} \text{h}^{-1} \text{bar}^{-1}$ )
Nexar from Thomas et al. <sup>22</sup>	52	$3.3 \pm 0.8$	$135.5 \pm 29$	$7.1 \times 10^{-3} \pm (1.5 \times 10^{-3})$
commercial PVA (DeltaMem 4155-30) as reported by Thomas et al. <sup>22</sup>	2.2	$1.0 \pm 0.2$	$32.8 \pm 5.9$	$7.2 \times 10^{-5}$
bare Nexar (UN)	$100 \pm 14$	$3.0 \pm (1.4 \times 10^{-4})$	$122.1 \pm 5.1$	$1.2 \times 10^{-1} \pm (1.4 \times 10^{-1})$
zwitterion coated (UZ)	$280 \pm 140$	$1.4 \pm (4.7 \times 10^{-3})$	$63.9 \pm 8.7$	$1.8 \times 10^{-2} \pm (5.1 \times 10^{-1})$

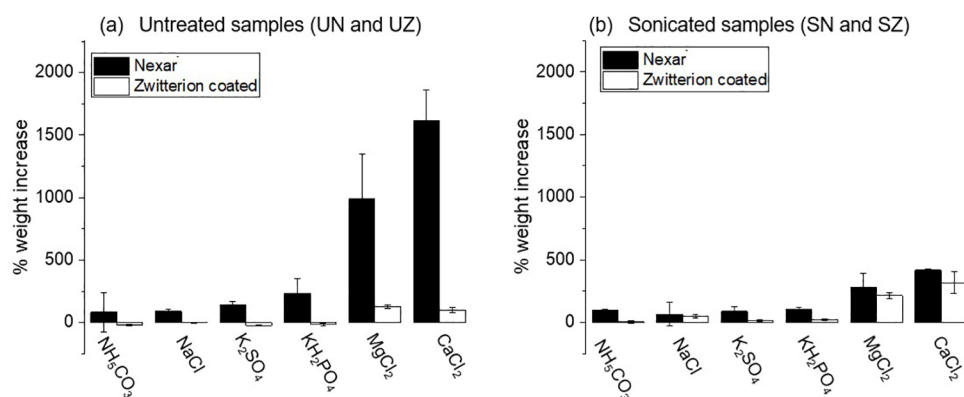


**Figure 6.** Scaling studies for both bare Nexar membranes and zwitterion-coated membranes during passive 7-day experiments, with the membranes desiccated prior to final weights measurement. Graph (a) shows unsonicated membranes placed into scaling solutions directly after being cast. Graph (b) shows membranes placed into scaling solutions after sonication. All scalant solutions are at their respective solubility limits in deionized water at 20 °C, with pH values in the 2.5–3.0 range. Coated membranes show a much higher resistance to scaling behavior. However, there is also mass loss occurring in the coated membranes in the left graph, which we identified as the washing away of unreacted polymerization precursors used in the coating process. Given the combination of scaling resistance and mechanical stability seen in the SZ and UZ samples, those present the optimal viability for moving forward with in future separation studies.

viable for testing in the system. We did not test the SZ membranes as sonication is not necessary for system implementation and would not likely be used for a practical membrane production for implementation; we only performed it to complete the gravimetric analysis we report and would not expect the flux value to be impacted by this membrane treatment.

The UZ (zwitterion-coated membranes) has a permeance that is 53% less than the UN membrane. Both membranes experience high amounts of salt removal, approaching 100% with error values on the order of  $10^{-3}$ . Under a one-way ANOVA with an alpha value of 0.05 and Tukey means comparison test, the salt removal values are not statistically different from each other. Likewise, the permeance (water transport property) is lower for the UZ membrane compared to the UN membrane. The addition of zwitterions into the polymer structure of membranes increases water transport properties when integrated into the polymer structure of membranes during initial casting.<sup>36–38</sup> The UZ membrane is a zwitterion copolymer coating on the surface of the base Nexar membrane (not integrated into the Nexar polymer during the initial casting). Since the zwitterions are added to the membrane surface via a polymerization reaction that also introduces other polymer species (HOMPP and PEGDA), the increased thickness of the membrane overall increases the transport resistance for the combination membrane. The permeability observed in Table 3 is consistent with these observations as that is the combined permeability of both the base membrane and the coating. All variations of experimental membranes, both previously studied Nexar, UN membranes in this study, and UZ membranes with the surface modifications had higher permeances than commercially available DeltaMem

pervaporation membranes that have a PVA active layer. While the PVA active layer is common for pervaporation membranes, these UZ and UN experimental membranes show higher levels of water transport when run in the same configuration. Future work to optimize the coating layer and decrease transport resistance could yield higher levels of flux, continuing to improve the performance of the system. The zwitterion coating is too brittle to be run independently in the pervaporation system, and thus, the composite (Nexar coated with the zwitterion polymer) membrane is the primary sample for analysis.

#### 4.2.2. Scaling Studies: UN and UZ Membrane Types.

Figure 6a shows the results of the passive scaling studies for the six individual scaling solutions described in Table 2 for the unsonicated bare Nexar (UN) membranes and the zwitterion-coated membranes (UZ). For all scalants, the UZ membranes have less mass gain at the end of the experiment than the UN, indicating less scalant deposited on the membrane surface. However, for four of the scalant solutions (ammonium bicarbonate, sodium chloride, potassium sulfate, and monopotassium phosphate), the observed membrane mass decreased during the passive scaling test time, with the largest membrane mass loss occurring in the sodium chloride samples at a level of  $-31.25\% \pm 2.54\%$ . This could result from (1) the low pH of the scaling solution degraded the membranes, (2) unreacted polymer from the coating process diffused out of the membrane during the week-long soaking, and/or (3) absorption of ambient moisture into the membranes during initial gravimetric analysis that is then removed in the later desiccation step. In the Supporting Information, we present three results of experiments designed to investigate our hypothesized sources of the mass loss observed in the passive

scaling tests of the membranes using desiccation, an acid soak, and sonication. Sonication of the as-synthesized membranes yielded the greatest amount of mass loss across all membrane samples, and therefore, this step was integrated into the subsequent studies. The mass loss in the actual studies is similar to what we saw with these membrane tests, which were also in the range of  $\sim 30\%$ , see *SI* for more information. While sonication may somewhat degrade bonded polymers, the continued presence of the coating on the surface and the anti-scaling behavior still present meant that the coating is still active on the surface.<sup>39</sup> Sonication is a facile step to integrate and “clean” the membranes prior to testing, and therefore, we implemented this to get a consistent baseline for testing.

**4.2.3. Scaling Studies: SN and SZ Membrane Types.** Figure 6b shows the results for the membranes after sonication and pre-scaling experiment removal of unreacted monomers. The zwitterion-coated membranes (SZ) had less scaling deposition on their surfaces than the uncoated membranes (UN). When looking back to the scaling studies lacking the sonication step, the bare Nexar membranes showed a high amount of scaling behavior, with weight percent increases on the order of 2000%. When sonicated, the coated membranes show weight percent increases consistently lower than 450%. When comparing the sonicated bare Nexar membranes to the sonicated zwitterion-coated membranes, however, there is no statistically significant difference in their scaling behavior; the sonicated bare Nexar (SN) membranes have weight percent increases like those in the sonicated zwitterion-coated membranes. We hypothesized that the sonication step impacted the structure of the Nexar polymer as previously described in the literature.<sup>24</sup>

Through studying both the coated and uncoated membranes in various states, we have more insight into the scaling behavior of the zwitterion-coated Nexar membranes. The SN membranes showed the smallest mass gain in the scaling studies; however, sonicated membranes may not be practical for pervaporation membrane use. This is because the sonication step in the SN membranes yielded brittle membranes that are unsuitable for use—these membranes cannot be manually handled and placed into the cross-flow pervaporation system without crumbling. While the UN membranes provide excellent separation and flux values, we observed the highest amount of scalant deposition in the passive scaling studies. The zwitterion-coated membranes are the most attractive option for future applications. The permeance values of the UZ membranes are less than the UN membranes, and this results from the extra coating in the UZ membranes that adds transport resistance. However, the reduction in scaling deposition in the UZ membranes is an excellent quality that has potential to enable longer term operation of the membranes. In the spaceflight applications we are interested in, a system balance between the speed of separation, the membrane lifetime, and the extent of recovery is vital. These studies necessitate future investigations into the kinetics of scaling so that operating conditions, maintenance schedules, and energy requirements for the full separation system can be determined. While the added resistance to transport will lower the speed of a given separation, the longer lifetime and excellent separation properties are worth making the tradeoff for as this will minimize resource use in these scenarios. Therefore, the combination of anti-scaling properties as well as mechanical stability provided by the zwitterion coatings on the Nexar membranes makes them an attractive option. While the sonication step (SZ) is necessary for the

gravimetric analysis of the scaling behavior of the membranes, sonication is not necessary for the system integration of the membrane as seen in the separation studies. Therefore, UZ is the most facile to produce and viable in system integration for future work.

## 5. CONCLUSIONS

In this paper, we have demonstrated the development of methods to deposit zwitterionic copolymers onto a membrane surface, the testing of these membranes in various separation and scaling scenarios, and the results of investigations into microstructure changes in Nexar polymers throughout this process. Overall, the increase in hydrophilicity provided by the zwitterion coating yields superior anti-scaling behavior when compared with the untreated Nexar membranes. While the sonicated Nexar membranes exhibit less scaling compared to their unwashed counterparts, the changes in microstructure of these membranes yield brittle behavior that results in them not being able to withstand manual handling or the pressure differentials of a separation system. Therefore, sonicating membranes is not a viable way of decreasing scaling behavior, and zwitterion coatings remain a much more attractive option. UN samples saw a maximum of 1500 wt % increase, whereas the SZ samples saw less than 500 wt % increase in the presence of calcium chloride, the highest scaling species present. Likewise, the other scalants had reductions in scaling phenomena between the UN and SZ samples. While flux is reduced somewhat due to the coating, the superior anti-scaling behavior makes the method an attractive option for system implementation due to reduced scaling and increased membrane lifetime. When it comes to membrane and system design, tradeoffs must occur between speed of a separation and system longevity and performance. For NASA applications, a longer timeline for a separation process is tolerable given a longer lifetime for the system that allows for more volume to be processed over the useful life of the membrane. The eventual goal of this vein of research is to utilize a passive treatment system that does not implement any energy inputs and, therefore, does not involve the stagnant deposition of scalant species on to the surface of the membrane. Our goal here was to understand passive scaling behavior on these membranes. These results continue to support the conclusion that the anti-scaling properties of the zwitterion-coated membranes are enhanced when compared to the Nexar membranes and continue to remain an attractive option for system implementation.

## ■ ASSOCIATED CONTENT

### Supporting Information

The Supporting Information is available free of charge at <https://pubs.acs.org/doi/10.1021/acsomega.2c08150>.

Further information regarding additional experimental protocols and results, detailing alternative polymerization methods, membrane swelling tests, and supplemental mass loss investigations, initial methods of zwitterion polymerization, water uptake in scalant solution testing protocol, water uptake test results, and mass loss investigations (PDF)

## AUTHOR INFORMATION

### Corresponding Author

Mary Laura Lind – School for Engineering of Matter, Transport and Energy, Arizona State University, Tempe, Arizona 85287, United States; NSF Nanosystems Engineering Research Center Nanotechnology-Enabled Water Treatment, Rice University, Houston, Texas 77005, United States; [orcid.org/0000-0001-8585-8054](https://orcid.org/0000-0001-8585-8054); Email: [mllind@asu.edu](mailto:mllind@asu.edu)

### Authors

Elisabeth R. Thomas – School for Engineering of Matter, Transport and Energy, Arizona State University, Tempe, Arizona 85287, United States; NSF Nanosystems Engineering Research Center Nanotechnology-Enabled Water Treatment, Rice University, Houston, Texas 77005, United States

Jae Sang Lee – School for Engineering of Matter, Transport and Energy, Arizona State University, Tempe, Arizona 85287, United States

Hoda Shokrollahzadeh Behbahani – School for Engineering of Matter, Transport and Energy, Arizona State University, Tempe, Arizona 85287, United States

Ani Nazari – School for Engineering of Matter, Transport and Energy, Arizona State University, Tempe, Arizona 85287, United States

Yusi Li – School for Engineering of Matter, Transport and Energy, Arizona State University, Tempe, Arizona 85287, United States; NSF Nanosystems Engineering Research Center Nanotechnology-Enabled Water Treatment, Rice University, Houston, Texas 77005, United States

Yi Yang – School for Engineering of Matter, Transport and Energy, Arizona State University, Tempe, Arizona 85287, United States

Matthew D. Green – School for Engineering of Matter, Transport and Energy, Arizona State University, Tempe, Arizona 85287, United States; [orcid.org/0000-0001-5518-3412](https://orcid.org/0000-0001-5518-3412)

Complete contact information is available at: <https://pubs.acs.org/10.1021/acsomega.2c08150>

### Notes

The authors declare no competing financial interest.

## ACKNOWLEDGMENTS

The authors would like to acknowledge support by the NSF Nanosystems Engineering Research Center for Nanotechnology-Enabled Water Treatment EEC-1449500. M.L.L. acknowledges support from NSF CAREER Award #CBET-1254215. E.R.T. was supported by a NASA Space Technology Research Fellowship 80NSSC19K1178 and by an ASU Graduate College tuition waiver. J.S.L. would like to acknowledge Army Research Office funding sources W911NF-18-1-0412 and W911NF-15-1-0353. M.D.G. and H.S.B. acknowledge support from NSF CBET 1836719. A.N. would like to acknowledge ASU's DAC polymer-enhanced cyanobacterial bioproductivity (AUDACity) award number DE-EE0009274. The authors acknowledge the use of facilities within the Eyring Materials Center at Arizona State University supported in part by NNCI-ECCS-2025490. Additionally, the authors thank Dr. Jill Williamson, of NASA's Marshall Spaceflight Center, for

providing information regarding spaceflight wastewater compositions.

## REFERENCES

- (1) Basile, A.; Figoli, A.; Khayet, M. *Fundamentals of Pervaporation*; In Woodhead Publishing Series in Energy; Woodhead Publishing, 2015.
- (2) Huang, R. Y. M. *Pervaporation Membrane Separation Processes*; Membrane science and technology series; Elsevier: Amsterdam, New York, 1991.
- (3) Schaetzel, P.; Bouallouche, R.; Ait Amar, H.; Nguyen, Q. T.; Riffault, B.; Marais, S. Mass Transfer in Pervaporation: The Key Component Approximation for the Solution-Diffusion Model. *Desalination* **2010**, *251*, 161–166.
- (4) Liang, B.; Zhan, W.; Qi, G.; Lin, S.; Nan, Q.; Liu, Y.; Cao, B.; Pan, K. High Performance Graphene Oxide/Polyacrylonitrile Composite Pervaporation Membranes for Desalination Applications. *J. Mater. Chem. A* **2015**, *3*, 5140–5147.
- (5) Khayet, M.; Matsuura, T. *Pervaporation and vacuum membrane distillation processes: Modeling and experiments - Khayet - 2004 - AIChE Journal - Wiley Online Library*. <https://aiche-onlinelibrary-wiley-com.ezproxy1.lib.asu.edu/doi/full/10.1002/aic.10161> (accessed May 26, 2020).
- (6) Shi, G. M.; Yang, T.; Chung, T. S. Polybenzimidazole (PBI)/Zeolitic Imidazolate Frameworks (ZIF-8) Mixed Matrix Membranes for Pervaporation Dehydration of Alcohols. *J. Membr. Sci.* **2012**, *415*–416, 577–586.
- (7) Kreiter, R.; Wolfs, D. P.; Engelen, C. W. R.; van Veen, H. M.; Vente, J. F. High-Temperature Pervaporation Performance of Ceramic-Supported Polyimide Membranes in the Dehydration of Alcohols. *J. Membr. Sci.* **2008**, *319*, 126–132.
- (8) Yadav, A.; Lind, M. L.; Ma, X.; Lin, Y. S. Nanocomposite Silicalite-1/Polydimethylsiloxane Membranes for Pervaporation of Ethanol from Dilute Aqueous Solutions. *Ind. Eng. Chem. Res.* **2013**, *52*, 5207–5212.
- (9) Kim, J.; Kim, H.-W.; Tijing, L. D.; Shon, H. K.; Hong, S. Elucidation of Physicochemical Scaling Mechanisms in Membrane Distillation (MD): Implication to the Control of Inorganic Fouling. *Desalination* **2022**, *527*, No. 115573.
- (10) Kochkodan, V.; Hilal, N. A Comprehensive Review on Surface Modified Polymer Membranes for Biofouling Mitigation. *Desalination* **2015**, *356*, 187–207.
- (11) Radu, A. I.; Bergwerff, L.; van Loosdrecht, M. C. M.; Picioreanu, C. A Two-Dimensional Mechanistic Model for Scaling in Spiral Wound Membrane Systems. *Chem. Eng. J.* **2014**, *241*, 77–91.
- (12) Benecke, J.; Rozova, J.; Ernst, M. Anti-Scale Effects of Select Organic Macromolecules on Gypsum Bulk and Surface Crystallization during Reverse Osmosis Desalination. *Sep. Purif. Technol.* **2018**, *198*, 68–78.
- (13) Tong, T.; Wallace, A. F.; Zhao, S.; Wang, Z. Mineral Scaling in Membrane Desalination: Mechanisms, Mitigation Strategies, and Feasibility of Scaling-Resistant Membranes. *J. Membr. Sci.* **2019**, *579*, 52–69.
- (14) Kaner, P.; Rubakh, E.; Kim, D. H.; Asatekin, A. Zwitterion-Containing Polymer Additives for Fouling Resistant Ultrafiltration Membranes. *J. Membr. Sci.* **2017**, *533*, 141–159.
- (15) Jaramillo, H.; Boo, C.; Hashmi, S. M.; Elimelech, M. Zwitterionic Coating on Thin-Film Composite Membranes to Delay Gypsum Scaling in Reverse Osmosis. *J. Membr. Sci.* **2021**, *618*, No. 118568.
- (16) Chiao, Y.-H.; Sengupta, A.; Chen, S.-T.; Huang, S.-H.; Hu, C.-C.; Hung, W.-S.; Chang, Y.; Qian, X.; Wickramasinghe, S. R.; Lee, K.-R.; Lai, J.-Y. Zwitterion Augmented Polyamide Membrane for Improved Forward Osmosis Performance with Significant Antifouling Characteristics. *Sep. Purif. Technol.* **2019**, *212*, 316–325.
- (17) Davenport, D. M.; Lee, J.; Elimelech, M. Efficacy of Antifouling Modification of Ultrafiltration Membranes by Grafting Zwitterionic Polymer Brushes. *Sep. Purif. Technol.* **2017**, *189*, 389–398.

- (18) Liu, C.; Lee, J.; Ma, J.; Elimelech, M. Antifouling Thin-Film Composite Membranes by Controlled Architecture of Zwitterionic Polymer Brush Layer. *Environ. Sci. Technol.* **2017**, *51*, 2161–2169.
- (19) Carter, L.; Wilson, L.; Orozco, N. Status of ISS Water Management and Recovery. In *41st International Conference on Environmental Systems*, 2011; p 11.
- (20) Carter, L. Status of the Regenerative ECLS Water Recovery System. In *40th International Conference on Environmental Systems*; American Institute of Aeronautics and Astronautics: Barcelona, Spain, 2010. DOI: 10.2514/6.2010-6216.
- (21) Carrasquillo, R. ISS Environmental Control and Life Support System (ECLSS) Future Development for Exploration, 2013. [https://www.nasa.gov/sites/default/files/files/issrdc\\_2013-07-17-1600\\_carrasquillo2013.pdf](https://www.nasa.gov/sites/default/files/files/issrdc_2013-07-17-1600_carrasquillo2013.pdf).
- (22) Thomas, E. R.; Jain, A.; Mann, S. C.; Yang, Y.; Green, M. D.; Walker, W. S.; Perreault, F.; Lind, M. L.; Verduzco, R. Freestanding Self-Assembled Sulfonated Pentablock Terpolymer Membranes for High Flux Pervaporation Desalination. *J. Membr. Sci.* **2020**, *613*, No. 118460.
- (23) Truong, P. V.; Black, R. L.; Coote, J. P.; Lee, B.; Ardebili, H.; Stein, G. E. Systematic Approaches To Tailor the Morphologies and Transport Properties of Solution-Cast Sulfonated Pentablock Copolymers. *ACS Appl. Polym. Mater.* **2019**, *1*, 8.
- (24) Truong, P. V.; Shingleton, S.; Kammoun, M.; Black, R. L.; Charendoff, M.; Willis, C.; Ardebili, H.; Stein, G. E. Structure and Properties of Sulfonated Pentablock Terpolymer Films as a Function of Wet–Dry Cycles. *Macromolecules* **2018**, *51*, 2203.
- (25) Inurria, A.; Cay-Durgun, P.; Rice, D.; Zhang, H.; Seo, D.-K.; Lind, M. L.; Perreault, F. Polyamide Thin-Film Nanocomposite Membranes with Graphene Oxide Nanosheets: Balancing Membrane Performance and Fouling Propensity. *Desalination* **2019**, *451*, 139.
- (26) Williamson, J. *Ersatz Urine and Urine Brine Procedures from NASA*, 2020.
- (27) Kelsey, L.; Pasadilla, P.; MacCallum, T.; Fisher, J. Development of Ionomer-Membrane Water Processor (IWP) Technology for Water Recovery from Urine. In *Th Int. Conf. Environ. Syst.*, 2014; p 23.
- (28) IR Spectrum Table. <https://www.sigmaaldrich.com/US/en/technical-documents/technical-article/analytical-chemistry/photometry-and-reflectometry/ir-spectrum-table#ir-table-by-compound> (accessed Apr 26, 2022).
- (29) Dai, Z.; Ansaloni, L.; Ryan, J. J.; Spontak, R. J.; Deng, L. Incorporation of an Ionic Liquid into a Midblock-Sulfonated Multiblock Polymer for CO<sub>2</sub> Capture. *J. Membr. Sci.* **2019**, *588*, No. 117193.
- (30) Moad, G.; Solomon, D. H. 2 - Radical Reactions. In *The Chemistry of Radical Polymerization (Second Edition)*; Moad, G., Solomon, D. H., Eds.; Elsevier Science Ltd: Amsterdam, 2005; pp 11–48. DOI: 10.1016/B978-008044288-4/50021-2.
- (31) Moad, G.; Solomon, D. H. 5 - Termination. In *The Chemistry of Radical Polymerization (Second Edition)*; Moad, G., Solomon, D. H., Eds.; Elsevier Science Ltd: Amsterdam, 2005; pp 233–278. DOI: 10.1016/B978-008044288-4/50024-8.
- (32) Yang, Y.; Ramos, T. L.; Heo, J.; Green, M. D. Zwitterionic Poly(Arylene Ether Sulfone) Copolymer/Poly(Arylene Ether Sulfone) Blends for Fouling-Resistant Desalination Membranes. *J. Membr. Sci.* **2018**, *561*, 69–78.
- (33) Angelini, A.; Fodor, C.; Yave, W.; Leva, L.; Car, A.; Meier, W. PH-Triggered Membrane in Pervaporation Process. *ACS Omega* **2018**, *3*, 18950–18957.
- (34) Lin, N. H.; Shih, W.-Y.; Lyster, E.; Cohen, Y. Crystallization of Calcium Sulfate on Polymeric Surfaces. *J. Colloid Interface Sci.* **2011**, *356*, 790–797.
- (35) Shaffer, D. L.; Tousley, M. E.; Elimelech, M. Influence of Polyamide Membrane Surface Chemistry on Gypsum Scaling Behavior. *J. Membr. Sci.* **2017**, *525*, 249–256.
- (36) Weng, X.; Ji, Y.; Zhao, F.; An, Q.; Gao, C. Tailoring the Structure of Polyamide Thin Film Composite Membrane with Zwitterions to Achieve High Water Permeability and Antifouling Property. *RSC Adv.* **2015**, *5*, 98730–98739.
- (37) Ni, L.; Meng, J.; Geise, G. M.; Zhang, Y.; Zhou, J. Water and Salt Transport Properties of Zwitterionic Polymers Film. *J. Membr. Sci.* **2015**, *491*, 73–81.
- (38) Wang, F.; Zheng, T.; Wang, P.; Chen, M.; Wang, Z.; Jiang, H.; Ma, J. Enhanced Water Permeability and Antifouling Property of Coffee-Ring-Textured Polyamide Membranes by In Situ Incorporation of a Zwitterionic Metal–Organic Framework. *Environ. Sci. Technol.* **2021**, *55*, 5324–5334.
- (39) Liu, Y.; Xie, L.; Ma, Y.; Xue, K.; Qiu, W.; Shan, T.; Gao, G. The Effects of Sonication Time and Frequencies on Degradation, Crystallization Behavior, and Mechanical Properties of Polypropylene. *Polym. Eng. Sci.* **2015**, *55*, 2566–2575.